Available online at www.sciencedirect.com
ScienceDirect
Journal of Magnetic Resonance 190 (2008) 316–326
JMR Journal of Magnetic Resonance
www.elsevier.com/locate/jmr

# Sensitivity enhancement in natural-abundance solid-state $^{33}$S MAS NMR spectroscopy employing adiabatic inversion pulses to the satellite transitions

Michael Ryan Hansen [a], Michael Brorson [b], Henrik Bildsøe [a], Jørgen Skibsted [a], Hans J. Jakobsen [a,*]

[a] *Instrument Centre for Solid-State NMR Spectroscopy, Interdisciplinary Nanoscience Center (iNANO), Department of Chemistry, University of Aarhus, DK-8000 Aarhus C, Denmark*
[b] *Haldor Topsøe A/S, Nymøllevej 55, DK-2800 Lyngby, Denmark*

Received 3 October 2007; revised 16 November 2007
Available online 21 December 2007

**Abstract**

The WURST (wideband uniform rate smooth truncation) and hyperbolic secant (HS) pulse elements have each been employed as pairs of inversion pulses to induce population transfer (PT) between the four energy levels in natural abundance solid-state $^{33}$S (spin $I = 3/2$) MAS NMR, thereby leading to a significant gain in intensity for the central transition (CT). The pair of inversion pulses are applied to the satellite transitions for a series of inorganic sulfates, the sulfate ions in the two cementitious materials ettringite and thaumasite, and the two tetrathiometallates $(NH_4)_2WS_4$ and $(NH_4)_2MoS_4$. These materials all exhibit $^{33}$S quadrupole coupling constants ($C_Q$) in the range 0.1–1.0 MHz, with precise $C_Q$ values being determined from analysis of the PT enhanced $^{33}$S MAS NMR spectra. The enhancement factors for the WURST and HS elements are quite similar and are all in the range 1.74–2.25 for the studied samples, in excellent agreement with earlier reports on HS enhancement factors (1.6–2.4) observed for other spin $I = 3/2$ nuclei with similar $C_Q$ values (0.3–1.2 MHz). Thus, a time saving in instrument time by a factor up to five has been achieved in natural abundance $^{33}$S MAS NMR, a time saving which is extremely welcome for this important low-$\gamma$ nucleus.


*Keywords:* $^{33}$S MAS NMR; Sensitivity enhancement; WURST and hyperbolic secant inversion pulses; Population transfer; Inorganic sulfates; Tetrathiometallates

## 1. Introduction

With sulfur being one of the most important elements in bio- and inorganic materials, it is unfortunate that NMR detection of the only NMR-active isotope for sulfur, i.e., $^{33}$S (spin $I = 3/2$ and 0.76% natural abundance), range among one of the greatest challenges in NMR spectroscopy of the NMR periodic table, albeit for obvious reasons [1]. This is clearly apparent from the few published $^{33}$S NMR studies, attributable to the low natural abundance of $^{33}$S coupled with its small magnetic moment, but probably also related to the extremely high-cost of isotopically enriched elemental $^{33}$S (or $^{33}$S materials). In particular this applies to solid-state $^{33}$S NMR studies, which have mainly been devoted to inorganic sulfates and sulfides [2–9]. Thus, any experimental or instrumental contribution which could improve "state-of-the-art" natural-abundance $^{33}$S MAS NMR would be very welcome. In recent solid-state NMR studies, we have demonstrated some basic S/N advancements in $^{33}$S MAS NMR by showing the possibilities and advantages in the observation of the spinning sidebands (ssbs) for the $^{33}$S satellite transitions at natural abundance, thereby allowing the determination of both the quadrupole coupling ($C_Q$ and $\eta_Q$) and the chemical shift anisotropy (CSA, $\delta_\sigma$ and $\eta_\sigma$) parameters from such spectra [7,9].

* Corresponding author. Fax: +45 8619 6199.
*E-mail address:* hja@chem.au.dk (H.J. Jakobsen).

1090-7807/$ - see front matter © 2007 Elsevier Inc. All rights reserved.
doi:10.1016/j.jmr.2007.11.014

Several new preparatory pulse elements have recently been introduced in solid-state NMR with the aim of increasing the signal intensity for the central transition (CT) in studies of half-integer quadrupolar nuclei using different population transfer (PT) schemes. These techniques include DFS (Double Frequency Sweeps) [10], RAPT (Rotor Assisted Population Transfer) [11], HS (hyperbolic secant) pulses [12,13], and finally the WURST (wideband uniform rate smooth truncation) technique [14] most recently used for spectral editing employing a highly selective WURST inversion pulse to a single ssb [15]. While DFS and RAPT make use of the intensity enhancement gained by saturation of energy-level populations for the satellite transitions, the HS and WURST pulse techniques employ selective population inversion between the energy levels, resulting in an increased PT and intensity enhancement for the CT. It is interesting to note that these solid-state NMR pulse elements may find their counterparts in the early days of basic liquid-state NMR. These include (i) the saturation effects of the homo- and heteronuclear Nuclear Overhauser Effect (NOE) [16], (ii) the homonuclear adiabatic Transitory Selective Irradiation (TSI) experiment by Hoffmann and Forsén [17], which is the precursor for (iii) the Selective Population Transfer (SPT) [18] and Double Selective Population Transfer (DSPT) [19] inversion-pulse experiments used for sensitivity enhancements and determination of relative signs of $J$ couplings.

In our continuous efforts to improve the sensitivity of solid-state $^{33}$S NMR, the present study demonstrates the sensitivity enhancement achieved by PT in natural abundance $^{33}$S MAS NMR employing a pair of inversion pulses (in some cases a single inversion pulse), either HS [13] or WURST [14], to the ssbs of the $^{33}$S satellite transitions. Signal enhancements (or gain in S/N ratios) by a factor of up to 2.25 have been achieved, using both pulse schemes, for the CT in a series of inorganic sulfates, tetrathiometallates, and two sulfate-containing cementitious materials (ettringite and thaumasite), which all have fairly small quadrupole couplings. This corresponds to a maximum saving by a factor of five in spectrometer time which is of great advantage in solid-state $^{33}$S MAS NMR considering the low-receptivity for this nucleus.

## 2. Experimental

### 2.1. Materials

All the simple inorganic sulfates ($NH_4Al(SO_4)_2 \cdot 12H_2O$, $KAl(SO_4)_2 \cdot 12H_2O$, $Na_2SO_4$, $K_2SO_4$, $(NH_4)_2SO_4$, $Rb_2SO_4$, $Cs_2SO_4$) are commercially available and were used without further purification. The two tetrathiometallates, $(NH_4)_2MoS_4$ and $(NH_4)_2WS_4$, are the same as recently synthesized and investigated by $^{33}$S MAS NMR [9]. The sample of ettringite, $[Ca_6Al_2(OH)_{12}](SO_4)_3 \cdot 26H_2O$, was synthesized using the same procedure as in an earlier $^{27}$Al MAS NMR study of this phase [20]. The purity of the sample was confirmed by powder XRD and $^{27}$Al MAS NMR, where the latter method shows the content of the thermodynamically stable monosulfate phase, $[Ca_4Al_2(OH)_{12}](SO_4) \cdot 6H_2O$, is less than 5 w/w%. The sample of thaumasite, $[Ca_3Si(OH)_6](SO_4)(CO_3) \cdot 12H_2O$, was prepared by decomposition of a sample of a $CaO–SiO_2–H_2O$ phase (C–S–H phase with $Ca/Si = 1.5$) obtained from a mixture of $CaCO_3$, $Ca(OH)_2$, and $Na_2SO_4$, stored at 5 °C and 95% RH for 720 days. A quantitative $^{29}$Si{$^1$H} CP/MAS NMR study [21] of the decomposed material shows that it contains $58 \pm 5$ w/w% thaumasite, the remaining being a C–S–H phase as judged from a $^{29}$Si MAS NMR spectrum.

### 2.2. NMR Spectroscopy

The $^{33}$S MAS NMR experiments were performed at 46.04 MHz on a Varian *Unity* INOVA-600 NMR spectrometer equipped with an Oxford Instruments 14.1T wide-bore magnet. The experiments employed a Varian Chemagnetics double-resonance T3® MAS probe for 7.5 mm rotors. The magic-angle was adjusted by MAS NMR of the nearby $^{14}$N frequency (43.04 MHz) using, e.g., a sample of $Pb(NO_3)_2$ as recently described [7]. Generally, the samples were spun at $\nu_r = 6.0$ kHz; however, some of the hydrated samples, in particular ettringite, showed a tendency to deteriorate (loss of $H_2O$) on prolonged spinning at 6 kHz because of frictional heating (at $\nu_r = 6.0$ kHz for this probe, the sample temperature is ~38 °C as recently shown [7]). Thus, for the hydrated samples $\nu_r = 3.0$ kHz was preferably used, along with ambient temperature (21 °C) air-flow through the probe to cool the stator. The rf field strengths were calibrated for different transmitter power levels using a 1.0 M aqueous solution of $Cs_2SO_4$ and usually a rf field strength of about 13 kHz, corresponding to a flip angle of 23°, was used for the PT inversion pulses and excitation of the enhanced and standard magnetization. This solution was also used as a secondary $^{33}$S chemical shift reference and has a chemical shift of 333 ppm relative to neat $CS_2$, the standard $^{33}$S chemical shift reference. The experimental conditions and setup are identical for the HS and WURST PT experiments. The two offset values used for the inversion pulses were set in the region of the two "horns" for the STs as recently proposed [13]. These positions were either calculated for samples with already determined $C_Q$, $\eta_Q$, $\delta_{iso}$ values [5–7] or estimated for the $SO_4^{2-}$ ions in the two cementitious samples (ettringite and thaumasite). In an estimation of the relaxation delays for the $SO_4^{2-}$ ions, we have taken advantage of the $T_1$ data determined for some inorganic sulfates [5]. The bandwidth of the HS and WURST inversion pulses was always set equal to the spinning frequency ($\nu_r$), while the pulse lengths ($T_P$) were in the range $T_P = 4$–12 ms and have been optimized to maximum enhancement performance for each sample, except for the two cementitious samples. It is noted that only minor differences in enhancement are observed for $T_P$ in the range $T_P = 4$–12 ms.

The HS and WURST (and also DFS and RAPT, not used here) shapes were generated using the spectrometer system wave form generator (WFG) hardware option along with either Varian's "Pandora's Box" software package or by direct programming of the individual preparatory pulse elements. The two offset values used for either inversion pulse shapes were generated by either cosine amplitude modulation (symmetrical offsets) or phase and amplitude modulation (non-symmetrical offsets) of the HS and WURST pulse shapes.

The signal-enhanced $^{33}$S MAS NMR spectra were analyzed, simulated and fitted to the experimental spectra by optimization of the quadrupole coupling, chemical shift, and experimental parameters, employing the most recently modified version of the STARS software package [22]. Some of the simulated spectra, presented in the figures along with the experiments, used these parameters which are summarized in Tables 1–3.

## 3. Results and discussion

Previous studies by the Wasylishen group [12,13] have demonstrated that the HS pulse shape apparently leads to somewhat higher sensitivity enhancements for spin $I = 3/2$ and 5/2 quadrupolar nuclei when compared to the DFS and RAPT methods. Thus, the present study of PT enhancement in $^{33}$S MAS NMR employed inversion pulses created by HS and WURST pulse shapes. The experimental conditions for the setup of the $^{33}$S PT enhancements (e.g., frequency offsets, rf field strengths, and bandwidths) followed the detailed descriptions for spin $I = 3/2$ nuclei recently summarized by Wasylishen and coworkers [13].

### 3.1. Simple inorganic sulfates

Selected examples illustrating the sensitivity enhancement for some simple inorganic sulfates, employing inversion pulses to specific ssbs in the satellite transitions of the $^{33}$S MAS NMR spectra, are shown in Figs. 1–3. To illustrate the spectral enhancements, the $^{33}$S MAS NMR spectra shown in these figures are acquired both without and with an inversion pulse prior to the single-pulse excitation and acquisition of the corresponding magnetizations under otherwise exactly identical experimental conditions.

The $^{33}$S MAS NMR spectra in Fig. 1 of $NH_4Al(SO_4)_2 \cdot 12H_2O$ without (Fig. 1a) and with (Fig. 1b) WURST PT serve as an excellent illustration of the methods presently being used for sensitivity enhancement of the CT by PT from the STs for half-integer quadrupolar nuclei in solids. The $^{33}$S quadrupole coupling constant ($C_Q$) for $NH_4Al(SO_4)_2 \cdot 12H_2O$ spinning at $\nu_r = 6.0$ kHz is only 106 kHz and is highly temperature dependent [7]. Thus, the ssbs for the satellite transitions are easily observed [7] as shown in Fig. 1a. Employing the WURST pulse scheme, these ssbs are nulled (or slightly negative) in return of a simultaneous gain in intensity (enhancement factor of 1.90) for the CT as illustrated in Fig. 1b. The HS pulse scheme gives an identi-

Table 1
$^{33}$S Enhancement factors, quadrupole coupling ($C_Q, \eta_Q$), and isotropic chemical shift ($\delta_{iso}$) parameters determined from natural abundance $^{33}$S MAS NMR for some simple inorganic sulfates employing HS and WURST inversion pulse PT experiments[a]

| Compound | Experiment | Scans | Enhancement factors | $C_Q$ (kHz) | $\eta_Q$ | $\delta_{iso}$ (ppm) | References |
|---|---|---|---|---|---|---|---|
| $NH_4Al(SO_4)_2 \cdot 12H_2O$ | WURST | 8192 | 1.90 | 106.1 | 0.05 | 330.4 | This work [7] |
| — | Standard | 44,000 | — | — | — | 331 | [5] |
| $KAl(SO_4)_2 \cdot 12H_2O$ | HS | 2048 | 1.75 | 633 | 0.20 | 331.8 | This work |
| — | WURST | 2048 | 1.83 | 638 | 0.17 | 331.8 | — |
| — | Standard | 295,000 | — | 638 | 0.04 | 331.5 | [7] |
| — | Standard | 268,000 | — | 640 | 0.16 | 331 | [5] |
| $Na_2SO_4$ | HS | 10,240 | 1.87 | 655 | 0.07 | 340.1 | This work |
| — | WURST | 10,240 | 1.74 | 655 | 0.01 | 340.2 | — |
| — | Standard | 214,000 | — | 660 | 0.13 | 341 | [5] |
| $K_2SO_4$ | HS | 8017 | 2.13 | 963 | 0.41 | 336.0 | This work |
| — | WURST | 8017 | 1.95 | 969 | 0.41 | 336.2 | — |
| — | Standard | 348,000 | — | 970 | 0.50 | 336 | [5] |
| $(NH_4)_2SO_4$ | HS | 8192 | 1.78 | 539 | 0.76 | 334.6 | This work |
| — | WURST | 8192 | 1.80 | 547 | 0.72 | 334.4 | This work |
| — | WURST[b] | 8192 | 1.64 | 539 | 0.75 | 334.5 | This work |
| — | Standard | 262,000 | — | 580 | 0.75 | 332 | [5] |
| $Rb_2SO_4$ | HS | 8192 | 2.25 | 860 | 0.39 | 336.4 | This work |
| — | WURST | 8192 | 1.97 | 869 | 0.38 | 336.7 | This work |
| — | Standard | 8192 | — | 855 | 0.42 | 336.2 | This work |
| — | Standard | 377,000 | — | 930 | 0.42 | 337 | [5] |
| $Cs_2SO_4$ | HS | 10,240 | 2.00 | 815 | 0.42 | 336.1 | This work |
| — | WURST | 10,240 | 1.92 | 810 | 0.36 | 335.8 | This work |
| — | Standard | 65,000 | — | 830 | 0.46 | 336 | [5] |

[a] The $C_Q$ values have error limits of ±5 kHz and the error limits for $\eta_Q$ are ±0.05. The $\delta_{iso}$ values are relative to neat $CS_2$ (the $S^{33}$ chemical shift of 1.0 M $Cs_2SO_4$ is 333 ppm relative to $CS_2$) and include corrections for the second-order quadrupolar shifts.
[b] This WURST experiment employed only a single offset value of 124.5 kHz.

Table 2
$^{33}$S Quadrupole coupling ($C_Q, \eta_Q$) and isotropic chemical shift ($\delta_{iso}$) parameters determined from natural abundance $^{33}$S MAS NMR for the two sulfate-containing cementitious materials ettringite, $[Ca_6Al_2(OH)_6](SO_4)_3 \cdot 26H_2O$, and thaumasite, $[Ca_3Si(OH)_6](SO_4)(CO_3) \cdot 12H_2O$, employing the WURST inversion pulse PT experiment[a]

| Compound | Scans/time (h) | $C_Q$ (kHz) | $\eta_Q$ | $\delta_{iso}$ (ppm) | References |
|---|---|---|---|---|---|
| Ettringite/S1 | 86,000/25 | 591 | 0.72 | 329.8 | This work |
| Ettringite/S2 | 86,000/25 | 810 | 0.97 | 329.6 | This work |
| Ettringite/S3 | 86,000/25 | 516 | 0.50 | 331.3 | This work |
| Ettringite[b] | 70,000/19 | 700 | 0.45 | 331 | [8] |
| Thaumasite | 162,000/48 | 950 | 0.33 | 330.9 | This work |

[a] The $C_Q$ values have error limits of ±5 kHz and the error limits for $\eta_Q$ are ±0.05. The $\delta_{iso}$ values are relative to neat $CS_2$ (the $^{33}$S chemical shift of 1.0 M $Cs_2SO_4$ is 333 ppm relative to $CS_2$) and include corrections for the second-order quadrupolar shifts.
[b] $^{33}$S MAS NMR spectrum recorded at 19.6T (63.6 MHz) without PT enhancement and analyzed using only a single site for the sulfate ions (see text).

Table 3
$^{33}$S Quadrupole coupling ($C_Q, \eta_Q$) and chemical shift parameters ($\delta_\sigma, \eta_\sigma, \delta_{iso}$) for $(NH_4)_2MS_4$ (M = W, Mo) determined from WURST/HS PT enhanced or standard natural abundance $^{33}$S MAS NMR spectra[a]

| Compound/sites | Experiment | Enhancement | $C_Q$ (kHz) | $\eta_Q$ | $\delta_\sigma$ (ppm) | $\eta_\sigma$ | $\delta_{iso}$ (ppm) | $\psi$ | $\chi$ | $\xi$ | References |
|---|---|---|---|---|---|---|---|---|---|---|---|
| $(NH_4)_2WS_4$ | | | | | | | | | | | |
| S(1), S(2) | WURST MAS | 2.04 | 705 | 0.76 | 390 | 0.05 | 542.0 | 153° | 11° | 2° | This work |
| S(1), S(2) | Standard MAS | 1 | 708 | 0.77 | 389 | 0.16 | 542.3 | 147° | 10° | 3° | [9] |
| S(3) | WURST MAS | 2.04 | 634 | 0.24 | 402 | 0.26 | 518.3 | 1° | 43° | 62° | This work |
| S(3) | Standard MAS | 1 | 620 | 0.14 | 396 | 0.35 | 518.7 | 87° | 47° | 73° | [9] |
| S(4) | WURST MAS | 2.04 | 533 | 0.10 | 387 | 0.00 | 495.8 | 54° | 15° | 87° | This work |
| S(4) | Standard MAS | 1 | 531 | 0.08 | 380 | 0.05 | 495.8 | 53° | 4° | 16° | [9] |
| $(NH_4)_2MoS_4$ | | | | | | | | | | | |
| S(av.) | HS MAS | 1.82 | — | — | 347 | 0.07 | 726.0 | 0° | 36° | 0° | This work |
| S(av.) | Standard MAS | 1 | 520 | 0.35 | 347 | 0.15 | 726.0 | 0° | 30° | 0° | [9] |

[a] The error limits for $C_Q$, $\eta_Q$, $\delta_\sigma$, and $\eta_\sigma$ are similar to those published earlier for the standard $^{33}$S MAS NMR spectra [9], i.e., ±0.07 kHz, ±0.05, ±4 ppm, and ±0.05, respectively. The $\delta_{iso}$ values are relative to neat $CS_2$ (the $^{33}$S chemical shift of 1.0 M $Cs_2SO_4$ is 333 ppm relative to $CS_2$) and include corrections for the second-order quadrupolar shifts. The $\psi$, $\chi$, $\xi$ Euler angles shown in the table are those directly obtained from the optimized fitting for the individual S-sites. The smallest error limits for these Euler angles are observed for the $\chi$ angle and are less than ±6°. The error limits for the $\psi$ and $\xi$ angles are much higher and could even be undefined for the small values of $\eta_Q$ and $\eta_\sigma$ [28].

cal spectrum and enhancement factor using the same experimental conditions. It is noted that employing the standard experimental conditions (e.g., frequency offsets, rf field strength) [13], generally used in this first application of PT enhancement to a low-receptive nucleus, enhancement factors approaching zero are observed (i.e., the CT is nulled) when the offsets are positioned at the "horns" of the ssbs in Fig. 1a. However, the sensitivity enhancement shown in Fig. 1b is achieved by moving the offsets to the outer regions of the manifold of ssbs. Clearly, with a rf field strength of ~13 kHz employed for the HS and WURST inversion pulses throughout the present study, these pulses induce PT for CTs with very small $C_Q$ values when applied to the "horns" for the STs as recently proposed for quadrupoles with much larger $C_Q$ and also higher rf fields [13]. Alternatively, it may be possible to achieve similar or even higher intensity enhancements by employing highly selective (i.e., low-power) inversion pulses to single ssbs, as recently used for spectral editing of different Rb sites in a mixture of Rb salts [15] with well-known quadrupole coupling parameters ($C_Q$ and $\eta_Q$).

The selected natural abundance $^{33}$S MAS NMR spectra in Fig. 2 illustrate the enhancements observed for the second-order lineshapes of the CTs in $Rb_2SO_4$, $K_2SO_4$, and $KAl(SO_4)_2 \cdot 12H_2O$ (K-Alum) employing the HS and WURST pulse schemes for comparison (see also Table 1). Experimental details and results are self-explanatorily from Fig. 2 and its figure caption. The largest enhancement observed in this study (i.e., 2.25) is obtained for the HS experiment on $Rb_2SO_4$ in Fig. 2b and its corresponding optimized simulated spectrum is shown in Fig. 2c.

The $^{33}$S MAS NMR spectra of $(NH_4)_2SO_4$ shown in Fig. 3 serve to illustrate the gain in CT intensity observed for different offsets applied to a $SO_4^{2-}$ ion with an asymmetry parameter $\eta_Q$ (~0.75) approaching 1, i.e., in particular when applied to the two "horns" close to the CT. A simulated MAS NMR spectrum ($\nu_r = 6000$ Hz), employing the quadrupole coupling parameters $C_Q = 543$ kHz and $\eta_Q = 0.74$, for $(NH_4)_2SO_4$, and showing the offsets for the three different HS and WURST PT experiments performed in Fig. 3, is shown in Fig. 4. From the experiments in Fig. 3 we find that the WURST experiment in Fig. 3h with offsets at the "horns" close to the CT highly suppresses the intensity for the CT (enhancement factor of 0.4) when compared to the HS experiment in Fig. 3d (enhancement factor of 1.44) for the same experimental conditions. However, it is also observed from Fig. 3 that by positioning the two off-

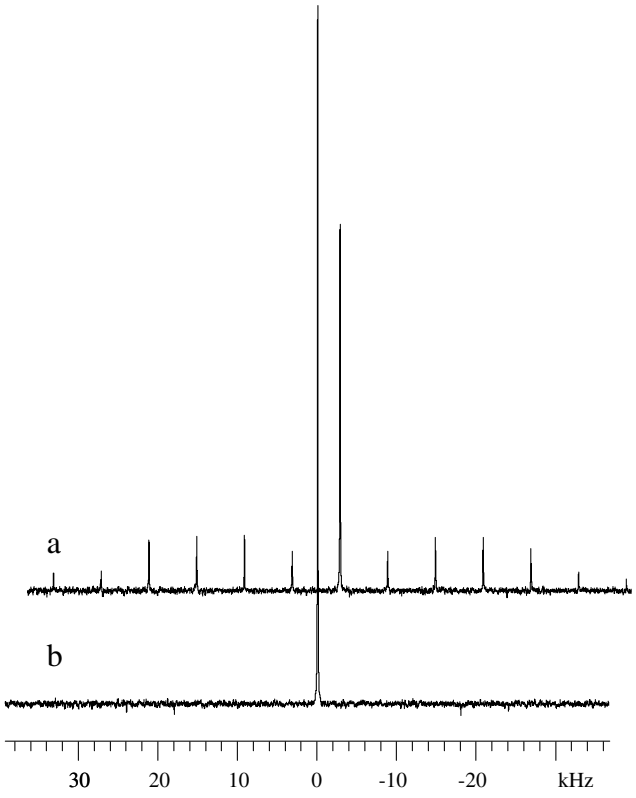


Fig. 1. Natural abundance $^{33}$S MAS NMR spectra (46.04 MHz at 14.1T, $\nu_r = 6000$ Hz) of $NH_4Al(SO_4)_2 \cdot 12H_2O$. Each spectrum used 8192 scans, a relaxation delay of 1 s, an acquisition time of 60 ms, total time of 2.4 h, a rf field strength of 13.2 kHz for both the WURST PT inversion pulse and single-pulse excitation (23° flip angle) of magnetization for (a) the standard (non-enhanced) and (b) the WURST PT enhanced spectrum. Offset values for the inversion pulses of ±38.9 kHz relative to the central transition (i.e., far outside the "horns" of the ssbs for the STs), a bandwidth of 6 kHz ($\nu_r = 6$ kHz), and $T_P = 4$ ms were used for the WURST experiment resulting in an enhancement factor of 1.90.

sets further away from the CT (see Fig 4), the enhancements for the HS and WURST pulse scheme are quite similar, slightly favoring the WURST experiment. Clearly, the populations for the CT become highly affected for the WURST experiment in Fig. 3h similar to the $^{33}$S WURST PT experiment for $NH_4Al(SO_4)_2 \cdot 12H_2O$ (*vide supra*).

The $^{33}$S MAS enhancement factors, following optimization of the enhanced spectra for the simple inorganic sulfate samples, are summarized in Table 1 along with the corresponding $C_Q$ and $\eta_Q$ values determined from their sensitivity enhanced spectra (see experimental section) and with those reported earlier [5–7]. From these data it is seen that the $^{33}$S enhancement factors for the inorganic sulfates fall in the range 1.74–2.25 with a trend that the larger enhancement factors are usually observed for the sulfates having the larger quadrupole coupling in the range $C_Q = 0.1$–$1.0$ MHz. For the individual sulfates the enhancement factors employing either HS or WURST pulses are quite similar, but generally with a slightly higher enhancement for HS compared to WURST. However, for a fair comparison we note that the HS pulse-shape experiments employed the optimized experimental conditions recently summarized for samples with already well-documented quadrupolar coupling parameters ($C_Q, \eta_Q$) and isotropic chemical shifts ($\delta_{iso}$) [13]. The corresponding $^{33}$S data are already known and taken into advantage for the optimization of the individual inorganic sulfates studied here [2.5–7]. The same experimental parameters used for the HS scheme were also employed in the WURST experiments without further detailed optimization for this pulse scheme.

Thus, for the simple inorganic sulfates investigated here with $C_Q$ ranging from 0.1 to 1.0 MHz, we have not been able to achieve the maximum enhancement factor of 2.6–2.7 obtained earlier [12,13] for other spin $I = 3/2$. However, this enhancement was achieved for $^{87}$Rb ($I = 3/2$) in $RbClO_4$ which has a much larger $C_Q$ (=3.3 MHz) [23]. The somewhat lower $^{33}$S enhancement factors determined here for the selected inorganic sulfates are nevertheless in good agreement with reported enhancements ranging from 1.6 to 2.4 [13] for other spin $I = 3/2$ nuclei in samples with $C_Q$ values in the range from 0.3 to 1.2 MHz. For example, for $^{23}$Na ($I = 3/2$) in $NaNO_3$ with $C_Q = 0.337$ MHz and $\eta_Q = 0.00$, an enhancement factor of only 1.6 was obtained [13]. A plausible explanation why a decrease of the enhancement factors is coupled to a decrease of the magnitude for $C_Q$ has already been addressed by Wasylishen and coworkers [13]. The proposed reason is that with a decrease in the magnitude of $C_Q$, the optimum position(s) for the offset of the inversion pulses [13] applied to the STs now starts perturbing the populations for the CT as we also clearly observe in this study and in particular for the $^{33}$S PT experiments described above for $NH_4Al(SO_4)_2 \cdot 12H_2O$ and $(NH_4)_2SO_4$.

In conclusion, for a series of selected simple inorganic sulfate with well-known $C_Q$ and $\eta_Q$ parameters ($C_Q = 0.1$–$1.0$ MHz), $^{33}$S PT enhancement factors ranging from 1.75 to 2.25 (i.e., corresponding to time saving factors of 3.0–5.0) have been observed employing the same standard rf field strengths for both HS [11–13] and WURST with similar or a slight advantage of the HS pulse scheme in case of samples with already known $C_Q$ and $\eta_Q$ parameters. However, we have noted that the WURST scheme generally appears less susceptible to the choice of the frequency positions for the two offset values. For that reason we have employed the WURST pulse scheme only to the two following cement-sulfate samples (ettringite and thaumasite) with unknown $C_Q$ and $\eta_Q$ parameters.

### 3.2. Ettringite and thaumasite

Ettringite and thaumasite are two sulfate-containing cementitious materials of unknown $^{33}$S $C_Q$, $\eta_Q$ parameters for the sulfate ions, but for both of which we earlier have performed extensive $^{27}$Al MAS [20] and $^{29}$Si{$^1$H} CP/MAS [21,24] NMR studies. The early single-crystal X-ray diffraction study [25] and the recent powder X-ray refinement [26] of the hexagonal ettringite structure (space group

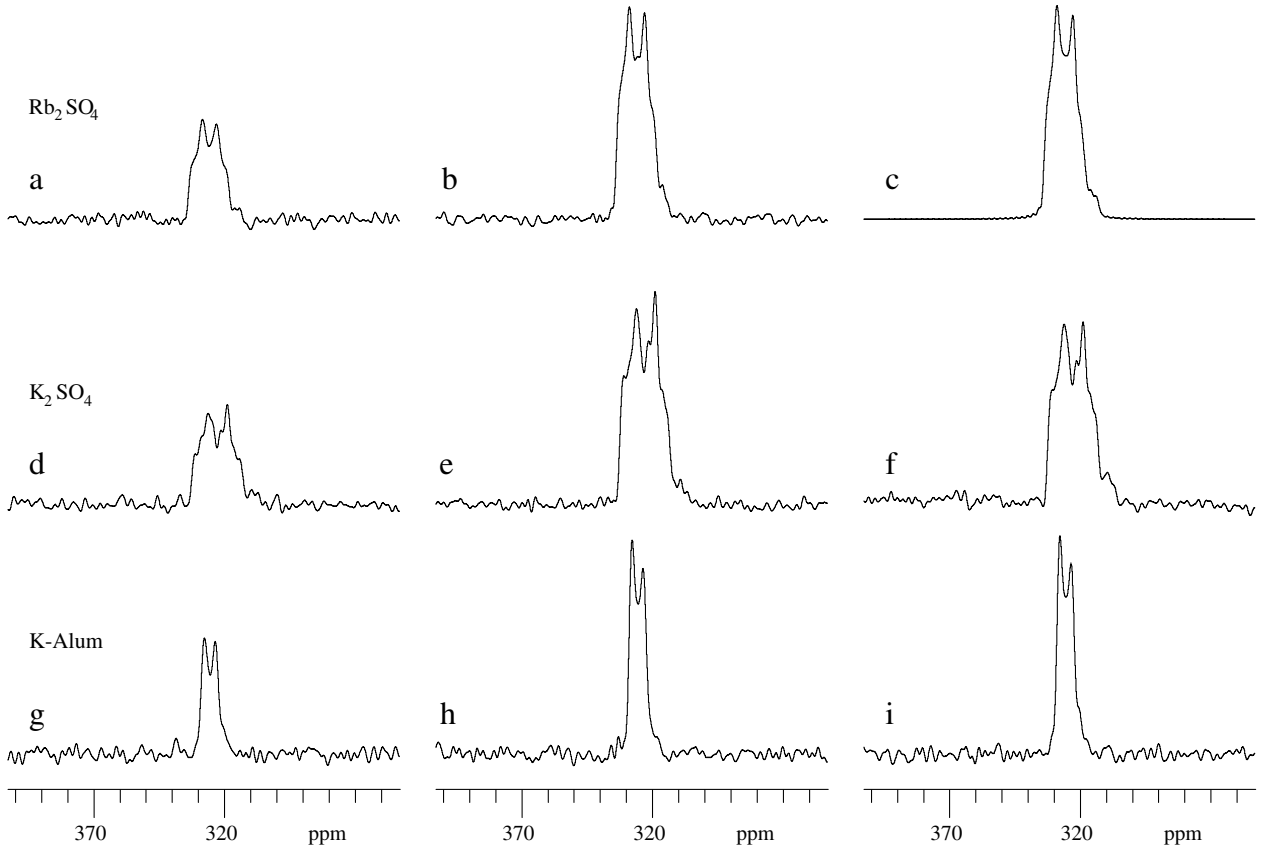


Fig. 2. Natural abundance $^{33}$S MAS NMR spectra ($\nu_r = 6000$ Hz) without and with selective PT HS/WURST inversion pulses for (a,b,c) $Rb_2SO_4$ in the upper row, (d,e,f) $K_2SO_4$ in the middle row, and (g,h,i) $KAl(SO_4)_2 \cdot 12H_2O$ (K-alum) in the lower-row. Left column (a,d,g) standard spectra without PT, middle column (b,e,h) HS PT spectra, and right column (f,i) WURST PT spectra. All PT experiments employed a rf field strength of 13.2 kHz for the HS and WURST inversion pulses and for the excitation (23° flip angle) of the standard and PT enhanced magnetization, a bandwidth of 6 kHz ($\nu_r = 6$ kHz), $T_P = 12$ ms. (a,b,c) $Rb_2SO_4$, each experimental spectrum (a,b) used 8192 scans, 4 s relaxation delay, 9.2 h, offsets 148.5 and −145.5 kHz, (b) HS enhancement factor 2.25, (c) simulation of the HS spectrum in (b) using the optimized parameters in Table 1. (d,e,f) $K_2SO_4$, each spectrum used 8017 scans, 4 s relaxation delay, 9.0 h, offsets 147.4 and −140.4 kHz, (e) HS enhancement factor 2.13, (f) WURST enhancement factor 1.95. (g,h,i) $KAl(SO_4)_2 \cdot 12H_2O$, each spectrum used 2048 scans, 1 s relaxation delay, 0.6 h, offsets 147.4 and −140.4 kHz, (h) HS enhancement factor 1.75, (i) WURST enhancement factor 1.83.

*P31c*) show that this phase includes three crystallographically independent sulfate ions, while thaumasite exhibits only a single $SO_4^{2-}$ crystallographic site according to single-crystal XRD [27].

### 3.3. Ettringite

The natural abundance $^{33}$S WURST PT MAS NMR spectrum of ettringite, $[Ca_6Al_2(OH)_6](SO_4)_3 \cdot 26H_2O$, acquired at 14.1T (46.04 MHz), $\nu_r = 3000$ Hz, 86,000 transients, and with a relaxation delay of 1 s (i.e., in a total time of 24 h), is shown in Fig. 5a and clearly indicates the presence of more than a single $SO_4^{2-}$ site. Offset values of 200 and −120 kHz are used for this sample, exhibiting unknown $C_Q$, $\eta_Q$ values for three distinct $SO_4^{2-}$ sites, and simply represent a first qualified guess based on the $SO_4^{2-}$ data in Table 1. Although no precise determination of the enhancement has been performed, we estimate the enhancement factors to be in the range of 1.6–2.0 for the three $SO_4^{2-}$ sites. Preparatory spectral simulations for the spectrum in Fig. 5a were performed using STARS with three different sites for the sulfate ions and were followed by simultaneous iterative fitting of the $SO_4^{2-}$ parameter ($C_Q, \eta_Q, \delta_{iso}$) sets for each of the three sites to the experimental spectrum employing an approximately 1:1:1 ratio. The resulting optimized parameters for each of the three sulfate ions in ettringite are summarized in Table 2 and the corresponding simulated three-site spectrum is shown in Fig. 5b. A good agreement between the simulated and experimental spectrum in Fig. 5 is observed. The $^{33}$S quadrupole coupling parameters ($C_Q, \eta_Q$) as well as the $^{33}$S isotropic shifts ($\delta_{iso}$) determined for the three structural non-equivalent sulfate ions in ettringite all fall in the range of the corresponding data determined elsewhere [2–8] and here for some simple inorganic sulfates.

During the course of this investigation the results of a high-field (19.6T, 63.6 MHz) natural abundance $^{33}$S MAS NMR study of ettringite, along with three already studied inorganic sulfates, have been reported [8]. The experimental spectrum of ettringite obtained in this high-field NMR study was analyzed and simulated using only a

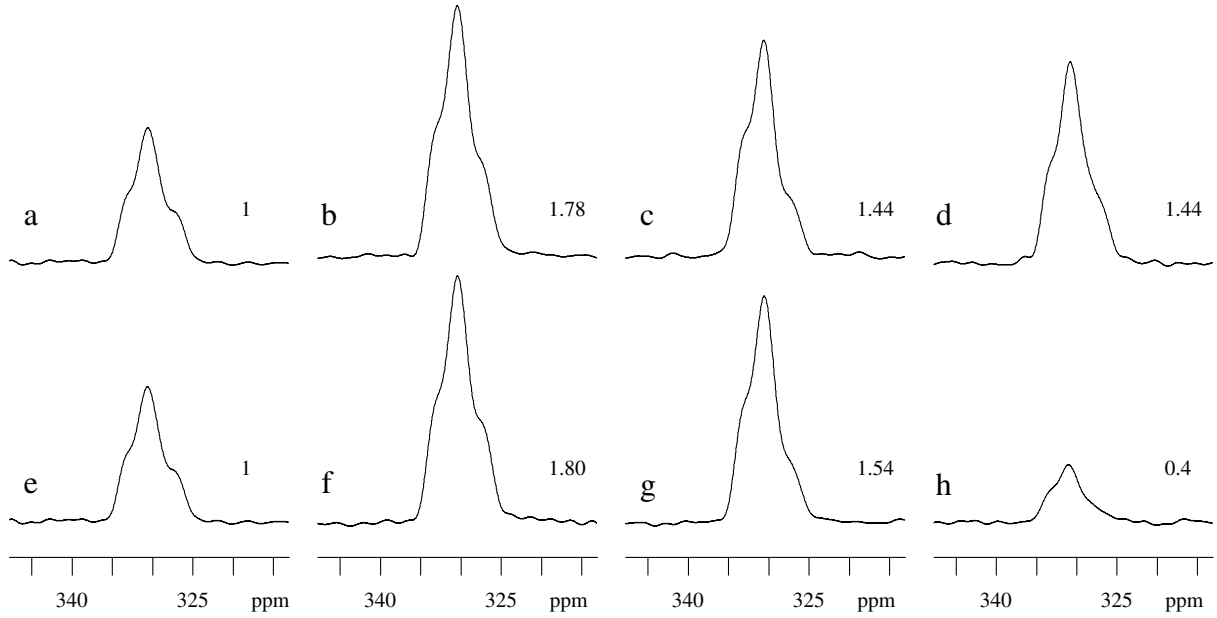


Fig. 3. Natural abundance $^{33}S$ MAS NMR spectra ($\nu_r = 6000$ Hz) of $(NH_4)_2SO_4$ illustrating the effect on the enhancement of applying HS and WURST inversion pulses at different offsets in the manifold of ssbs for the STs. Upper row (a, b, c, d) illustrates the effects for the HS experiments while the lower-row (e, f, g, h) are the results of the WURST PT enhancements. All PT experiments employed a rf field strength of 13.2 kHz for the HS and WURST inversion pulses and for the excitation (23° flip angle) of the standard and PT enhanced magnetizations, a bandwidth of 6 kHz, $T_P = 12$ ms, a relaxation delay of 2 s, and 8192 scans (4.6 h each spectrum). A standard spectrum without PT is shown in (a) and (e). Identical offset values are employed for the HS and WURST spectra positioned vertically. The offsets are (b, f) 124.5 and −122.5 kHz, (c, g) 220.5 and −218.5 kHz, (d, h) 45.5 and −44.5 kHz, and correspond to the arrows indicated in Fig. 4. The numbers to the right of the spectra are the enhancement relative to the standard spectra.

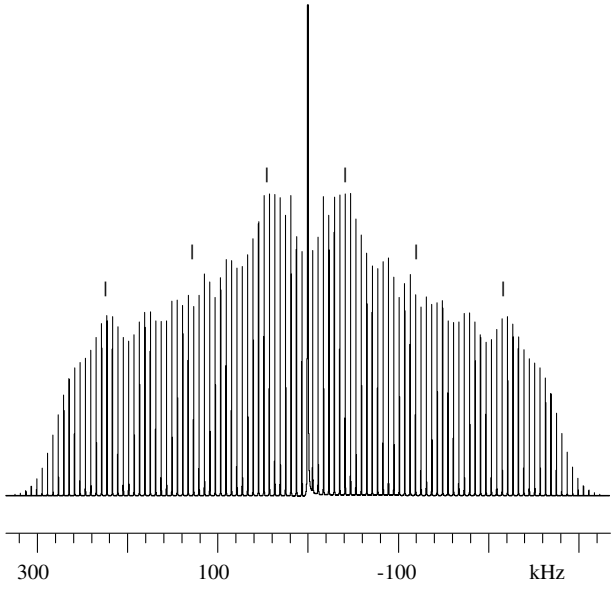


Fig. 4. Simulated $^{33}S$ MAS NMR spectrum of $(NH_4)_2SO_4$, employing $C_Q = 543$ kHz and $\eta_Q = 0.71$, and showing the manifold of ssbs for the satellite transitions. The kHz scale is relative to the primary external reference of 1.0 M $Cs_2SO_4$. The pairs of vertical bars positioned nearly symmetrical around the central transition (which clearly has been cut-off in the figure) correspond to the offsets given in the caption of Fig. 3.

single $SO_4^{2-}$ site, although the resemblance between the experimental and simulated spectrum is not convincing [8]. Moreover, we note that the crystal structure data show the presence of three non-equivalent $SO_4^{2-}$ ions in the asymmetric unit [24]. Considering the line-narrowing effect of the second-order quadrupolar broadening for the CT with increasing magnetic field strength, it obviously would be of interest to compare the published experimental high-field (19.6T, 63.6 MHz) $^{33}S$ MAS NMR spectrum (Fig. 2 in reference [8]) with the corresponding high-field simulated spectrum employing the three sets of parameters ($C_Q, \eta_Q, \delta_{iso}$) determined in the present study at 14.1T (46.04 MHz) for the three different $SO_4^{2-}$ sites in ettringite (Table 2). This 63.6 MHz three-site simulated $^{33}S$ MAS NMR spectrum is shown in Fig. 5c and exhibits features quite similar to those seen in the experimental spectrum [8], e.g., the shoulder observed to low-frequency (~325 ppm) from the main resonance(s). In particular, we also note that the total widths of the CT resonances, both excluding and including the low-frequency shoulder, are similar for the experimental and simulated spectrum, i.e., ~9.0 ppm, excluding and ~13.3 ppm, including the shoulder.

In conclusion, this exercise on ettringite has clearly demonstrated that although the use of the highest possible magnetic field may be of advantage for sensitivity and line-narrowing reasons, it may under certain circumstances limit resolution in case of overlapping resonances from different sites. This could make the analysis and extraction of spectral parameters difficult or even impossible. As illustrated here combining the results from spectra acquired at two (or at least two) different magnetic fields is preferable in such cases.

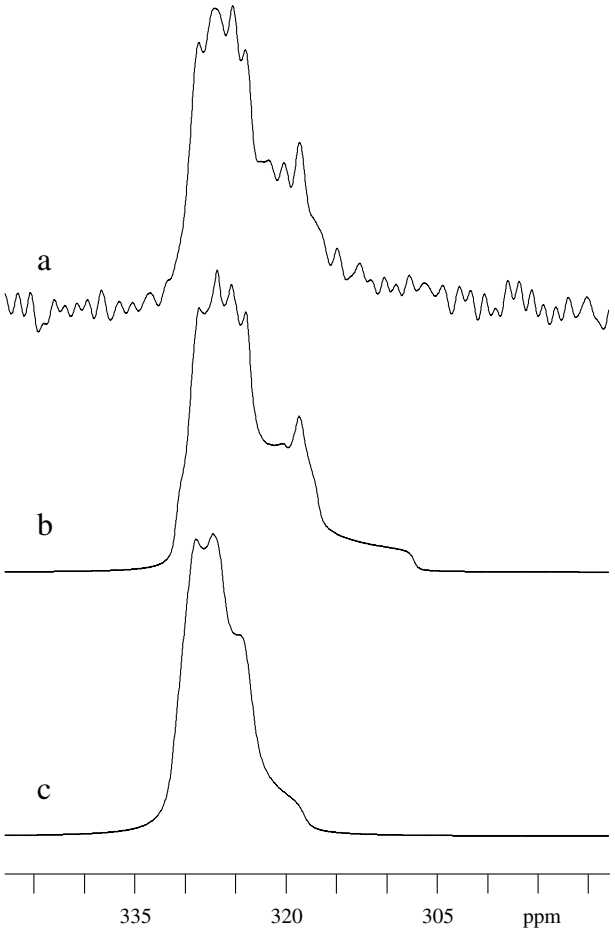


Fig. 5. (a) Experimental WURST PT and (b) simulated 46.04 MHz (14.1T) $^{33}$S MAS NMR spectra of ettringite. (c) Simulated 63.5 MHz (19.6T) spectrum employing the parameters for the three distinct $SO_4^{2-}$ sites determined from the 46.04 MHz spectrum in (a) and listed in Table 2.

### 3.4. Thaumasite

The natural abundance $^{33}$S WURST PT MAS NMR spectrum of thaumasite, $[Ca_3Si(OH)_6](SO_4)(CO_3) \cdot 12H_2O$, $\nu_r = 3000$ Hz, 162,000 transients, and also with a relaxation delay of 1 s, is shown in Fig. 6. The offset values, 200 and −120 kHz, are the same as used for ettringite. The almost doubling of the time required for this spectrum compared to that of ettringite (Fig. 5) can be justified by the higher ratio for the $SO_4^{2-}$ ions in ettringite versus thaumasite (ratio of 1.5:1) for molecular formulas of almost identical weights, combined with a purity of only 60 w/w% for the thaumasite sample. In accordance with the crystal structure determined by powder XRD for thaumasite [25], simulations combined with iterative fitting to the experimental spectrum show that this spectrum can be fitted satisfactory (Fig. 6b), using only a single set of parameters for this sample. The final $^{33}$S parameters corresponding to the optimized fit in Fig. 6b are summarized in Table 2 and are of the same magnitude as the $^{33}$S quadrupole coupling and chemical shift parameters determined here and earlier for $SO_4^{2-}$ ions in simple inorganic sulfates [2–8].

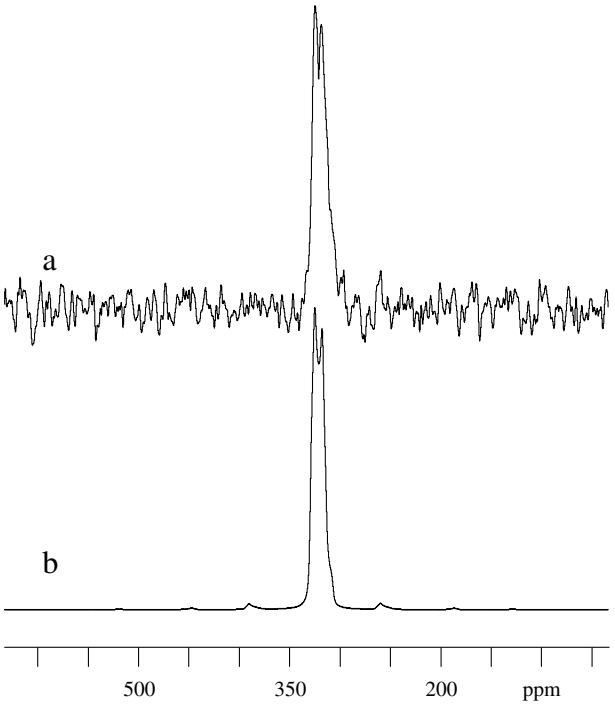


Fig. 6. (a) Experimental WURST PT and (b) simulated 46.04 MHz $^{33}$S MAS NMR spectra of thaumasite. See Table 2 and the text for details.

### 3.5. $(NH_4)_2WS_4$ and $(NH_4)_2MoS_4$

The PT $^{33}$S MAS NMR enhancements, illustrated above for $SO_4^{2-}$ ions in inorganic sulfates and two cementitious materials, will now finally also be applied to the recently published satellite transitions observed in the standard $^{33}$S MAS NMR spectra for the two ammonium tetrathiometallates $(NH_4)_2MS_4$ (M = W and Mo) [9] employing both WURST and HS inversion pulses. It should be emphasized that the determination of precise $^{33}$S quadrupole coupling parameters for the transition-metal M = S bonds in these samples from their $^{33}$S MAS NMR spectra, for which the CTs are dominated by fairly large $^{33}$S CSAs, would only have been possible through the observation of the $^{33}$S STs [9].

### 3.6. $(NH_4)_2WS_4$

For $(NH_4)_2WS_4$ two offset values, 120.8 kHz and −107.2 kHz, estimated from the published satellite transition spectra [9] were employed for both the WURST and HS $^{33}$S PT MAS NMR enhancement spectra and compared to a standard spectrum without PT using otherwise identical experimental conditions. The $^{33}$S PT enhancement factors for the WURST (2.04) and HS (1.99) experiments, employing these two offset values, are identical and correspond to a time saving by a factor of four. An expansion of the originally observed natural abundance $^{33}$S MAS NMR spectrum (without PT) for the CTs in $(NH_4)_2WS_4$ is shown in Fig. 7a along with the correspondingly fitted spectrum in Fig. 7b for the three crystallographically

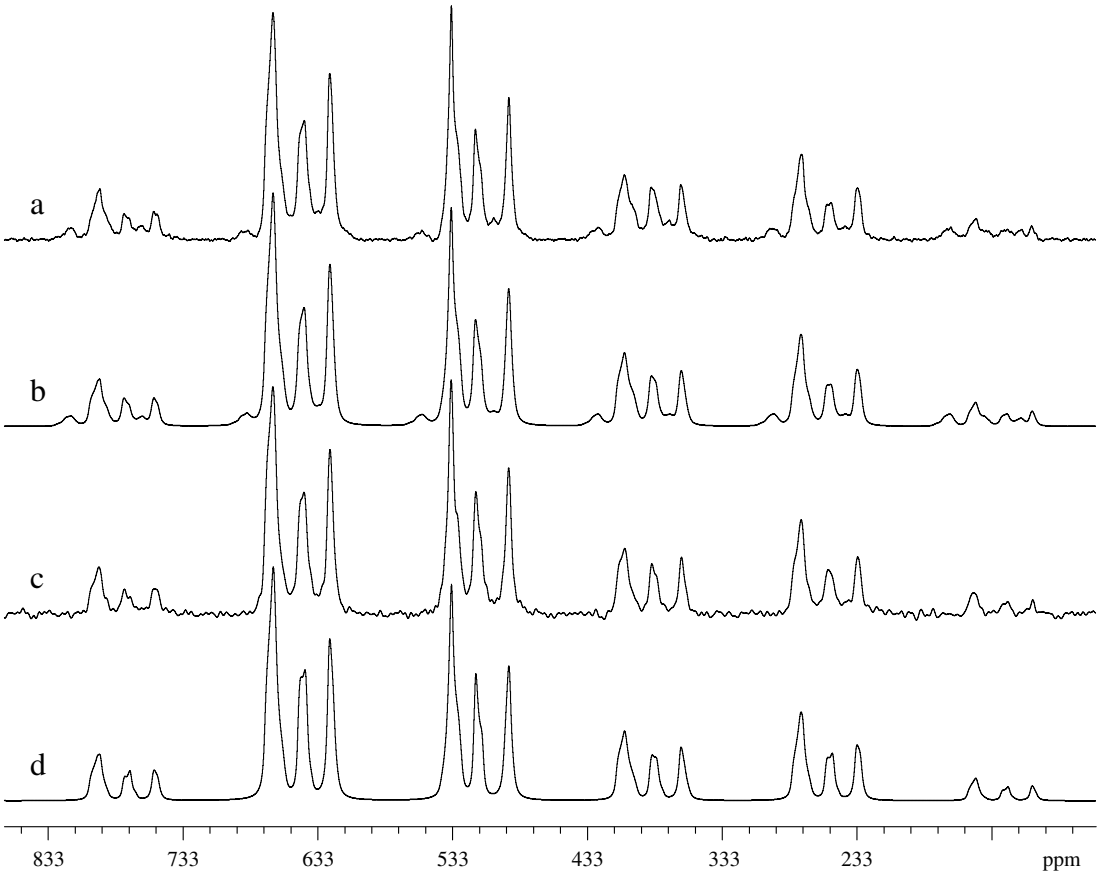


Fig. 7. (a) Experimental and (b) simulated 46.04 MHz $^{33}$S MAS NMR spectra of $(NH_4)_2WS_4$, originally observed (316,000 scans, 1 s relaxation delay, 3.7 days) and simulated using single-pulse excitation for the observation of both the CTs and STs [9]; see Table 3 and text. (c) Experimental 46.04 MHz WURST PT $^{33}$S MAS NMR spectrum observed for the CTs in $(NH_4)_2WS_4$ (30,700 scans, 1 s relaxation delay, 8,5 h); see Table 3 and text. (d) Optimized simulation for the $^{33}$S MAS NMR spectrum of the CTs in $(NH_4)_2WS_4$ based on the WURST PT spectrum in (c) based on the final parameters listed in Table 3. Note the absence of the resonances for the STs in spectra (c) and (d), when compared to the spectra in (a) and (b), respectively. The value $\delta = 333$ ppm on the ppm scale corresponds to $\delta = 0$ ppm for the secondary $^{33}$S chemical shift reference of 1.0 M $Cs_2SO_4$ used elsewhere [9].

non-equivalent S-sites (values shown in Table 3 are taken from reference [9]). For comparison the same expansion observed for the WURST PT $^{33}$S MAS NMR spectrum is displayed in Fig. 7c and the optimized simulation for this spectrum is shown in Fig. 7d. A strikingly good agreement is observed for the second-order lineshapes of the individual resonances in the spectra for the two different experiments. Thus, the HS and WURST PT pulse schemes appear robust towards CT second-order lineshapes even in case the CT is dominated by CSA. Furthermore, it is also seen that the low-intensity resonances arising from the STs, and observed in the standard MAS spectrum (Fig. 7a), are nulled in the WURST PT spectrum (Fig. 7c). Most importantly, it is noted that whereas, the spectrum in Fig. 7a was acquired using 316,000 transients and a relaxation delay of 1 s (3.7 days), the PT spectrum in Fig. 7c only required 30,700 transients with a 1 s relaxation delay (8.5 h), and with the spectra exhibiting a fairly similar S/N level. The optimized simulation in Fig. 7d used our recently determined values [9] as starting parameters for the quadrupole coupling $(C_Q, \eta_Q)$ and chemical shift $(\delta_\sigma, \eta_\sigma, \delta_{iso})$ tensorial interactions, including the three Euler angles $(\psi, \chi, \xi)$ describing the relative orientation of these tensors, in a fit to the experimental CT spectrum in Fig. 7c. The final parameters corresponding to the optimized simulation in Fig. 7d are summarized in Table 3 along with the corresponding parameters reported recently [9] and determined employing both the $^{33}$S ST and CT spectra in the fitting procedure. From the data in Table 3 it is seen that the parameters determined here, solely from the CTs and their second-order lineshapes, agree within error limits with those reported earlier [9].

### 3.7. $(NH_4)_2MoS_4$

Similar to the discussion above for $(NH_4)_2WS_4$, the complete $^{33}$S ST/CT MAS NMR spectrum recorded for $(NH_4)_2MoS_4$ [9] formed the basis for the performance of PT $^{33}$S MAS NMR enhancement spectra for this material. The two offset values 90.4 kHz and –89.6 kHz, estimated from the $^{33}$S ST MAS spectrum [9], were employed for both the HS and WURST PT $^{33}$S MAS experiment. These two experiments also gave an identical enhancement factor of 1.80 (±0.02), which is illustrated here in Fig. 8 for the

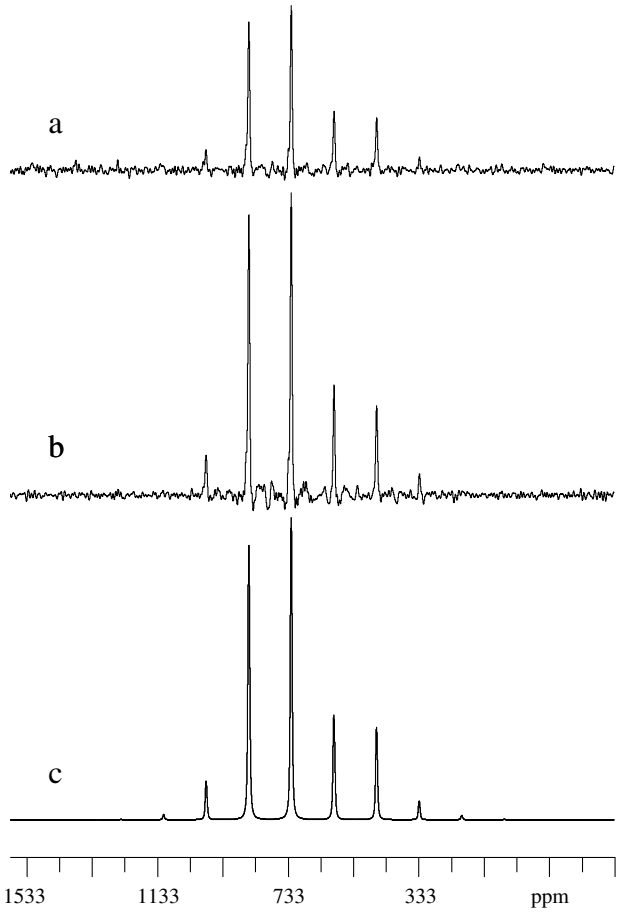


Fig. 8. Natural abundance $^{33}$S MAS NMR spectra ($\nu_r = 6000$ Hz) of $(NH_4)_2MoS_4$ displayed on an absolute intensity scale for (a) without PT and (b) with HS PT which corresponds to an enhancement factor of 1.8 based on integrated intensities. Both spectra were observed using single-pulse excitation and identical experimental conditions, i.e., 48,000 scans, 1 s relaxation delay, 13.3 h. (c) Simulation based on the HS PT $^{33}$S MAS NMR spectrum in (b) and the optimized parameters listed in Table 3. The S/N level for the PT enhanced spectrum in (b) compares favorably with that of the earlier published spectrum [9], which required 182,000 scans and 50.5 h. These spectra both show the same "impurity" resonances in the center part of the CT. The value $\delta = 333$ ppm on the ppm scale corresponds to $\delta = 0$ ppm for the secondary $^{33}$S chemical shift reference of 1.0 M $Cs_2SO_4$ used elsewhere [9].

HS PT $^{33}$S MAS experiment using 48,000 transients and a relaxation delay of 1 s. Thus, the time of 13.3 h required to achieve the HS PT $^{33}$S CT MAS spectrum in Fig. 8b compares favorably with the time of 50.5 h (182,000 transients and a 1 s relaxation delay) used for the recently reported spectrum. In order to arrive at the optimized fit (Fig. 8c) for the experimental spectrum (Fig. 8b), the $C_Q$, $\eta_Q$ values determined earlier from the $^{33}$S ST spectrum [9] were employed as fixed values in the optimization. The reason these parameters could not be varied is that no second-order lineshapes are observed even in the 14.1T $^{33}$S resonances for the CT in $(NH_4)_2MoS_4$. The values obtained from the optimization for the chemical shift parameters ($\delta_\sigma, \eta_\sigma, \delta_{iso}$) are summarized in Table 3 and are almost identical to those determined earlier (also listed in Table 3).

In conclusion, for the two transition-metal tetrathiometallates investigated here with $C_Q$ in the range 0.5–0.7 MHz, PT enhancement factors from 1.8 to 2.0 employing either WURST or HS inversion pulses to the STs have been achieved for their $^{33}$S CTs. Thus, the enhancement factors for these CTs, which are dominated by $^{33}$S CSA interactions, are quite similar to those obtained for $SO_4^{2-}$ ions of similar $C_Q$ value.

## 4. Conclusions

Significant sensitivity enhancements have been achieved by population transfer (PT) from the satellite transitions (STs) into the central transition (CT) employing either WURST or HS inversion pulses in natural abundance $^{33}$S (spin $I = 3/2$) MAS NMR spectra of sulfate ions and tetrathiometallates with $C_Q$ in the range 0.1–1.0 MHz. The observed enhancement factors are all in the range of 1.74–2.25 for the studied samples in excellent agreement with earlier reports on HS enhancement factors (1.6–2.4) observed for other spin $I = 3/2$ nuclei with similar $C_Q$ values (0.3–1.2 MHz) [13]. Finally, with the uncertainty in mind of estimating quadrupole coupling parameters for samples with unknown $C_Q$, $\eta_Q$ values, we have found the enhancements for the WURST inversion pulse method to be less sensitive to the requirement of an a priori knowledge of the $C_Q$, $\eta_Q$ values.

## Acknowledgments

The use of the facilities at the Instrument Centre for Solid-State NMR Spectroscopy, University of Aarhus, sponsored by the Danish Natural Science Research Council, the Danish Technical Science Research Council, Teknologistyrelsen, Carlsbergfondet, and Direktør Ib Henriksens Fond is acknowledged.

## References

[1] K.J.D. MacKenzie, M.E. Smith, Multinuclear Solid-State NMR of Inorganic Materials, Pergamon Press, Oxford, 2002.
[2] H. Eckert, J.P. Yesinowski, Sulfur-33 NMR at natural abundance in solids, J. Am. Chem. Soc. 108 (1986) 2140–2146.
[3] W.A. Daunch, P.L. Rinaldi, Natural-abundance solid-state $^{33}$S NMR with high-speed magic-angle spinning, J. Magn. Reson. A123 (1996) 219–221.
[4] T.A. Wagler, W.A. Daunch, P.L. Rinaldi, A.R. Palmer, Solid state $^{33}$S NMR of inorganic sulfides, J. Magn. Reson. 161 (2003) 191–197.
[5] T.A. Wagler, W.A. Daunch, M. Panzer, W.J. Youngs, P.L. Rinaldi, Solid-state $^{33}$S MAS NMR of inorganic sulfates, J. Magn. Reson. 170 (2004) 336–344.
[6] S. Couch, A.P. Howes, S.C. Kohn, M.E. Smith, $^{33}$S solid state NMR of sulfur speciation in silicate glasses, Solid State Nucl. Magn. Reson. 26 (2004) 203–208.
[7] H.J. Jakobsen, A.R. Hove, H. Bildsøe, J. Skibsted, Satellite transitions in natural abundance solid-state $^{33}$S MAS NMR of alums—Sign change with zero-crossing of $C_Q$ in a variable temperature study, J. Magn. Reson. 180 (2006) 170–177.
[8] J.P. d'Espinose de Lacaillerie, F. Barberon, B. Bresson, P. Fonollosa, H. Zanni, V.E. Fedorov, N.G. Naumov, Z. Gan, Applicability of

natural abundance $^{33}S$ solid-state NMR to cement chemistry, Cem. Concr. Res. 36 (2006) 1781–1783.

[9] H.J. Jakobsen, A.R. Hove, H. Bildsøe, J. Skibsted, M. Brorson, Advancements in natural abundance solid-state $^{33}S$ MAS NMR: characterization of transition-metal M = S bonds in ammonium tetrathiometallates, Chem. Commun. (2007) 1629–1631.

[10] A.P.M. Kentgens, R. Verhagen, Advantages of double frequency sweeps in static, MAS and MQMAS NMR of spin $I = 3/2$ nuclei, Chem. Phys. Lett. 300 (1999) 435–443.

[11] Z. Yao, H.-T. Kwak, D. Sakellariou, L. Emsley, P.J. Grandinetti, Sensitivity enhancement of the central transition NMR signal of quadrupolar nuclei under magic-angle spinning, Chem. Phys. Lett. 327 (2000) 85–90.

[12] R. Siegel, T.T. Nakashima, R.E. Wasylishen, Signal enhancement of NMR spectra of half-integer quadrupolar nuclei in solids using hyperbolic secant pulses, Chem. Phys. Lett. 388 (2004) 441–445.

[13] R. Siegel, T.T. Nakashima, R.E. Wasylishen, Sensitivity enhancement of NMR spectra of half-integer spin quadrupolar nuclei in solids using hyperbolic secant pulses, J. Magn. Reson. 184 (2007) 85–100, and references cited therein to various versions of the DFS, RAPT, and HS techniques.

[14] E. Kupce, R. Freeman, Adiabatic pulses for wideband inversion and broadband decoupling, J. Magn. Reson. A115 (1995) 273–276.

[15] K.K. Dey, S. Prasad, J.T. Ash, M. Deschamps, P.J. Grandinetti, Spectral editing in solid-state MAS NMR of quadrupolar nuclei using selective satellite inversion, J. Magn. Reson. 185 (2007) 326–330.

[16] (a) I. Solomon, Relaxation processes in a system of two spins, Phys. Rev. 99 (1955) 559–565;
(b) D. Neuhaus, M.P. Williamson, The Nuclear Overhauser Effect in Structural and Conformational Analysis, VCH, New York, 1989.

[17] R.A. Hoffman, S. Forsén, Double resonance experiments, in: J.W. Emsley, J. Feeney, L.H. Sutcliffe (Eds.), Progress in Nuclear Magnetic Resonance Spectroscopy, vol. 1, Pergamon Press, Oxford, 1966, pp. 34–87.

[18] H.J. Jakobsen, S.Aa. Linde, S. Sørensen, Sensitivity enhancement in $^{13}C$ FT NMR from selective population transfer (SPT) in molecules with degenerate proton transitions, J. Magn. Reson. 15 (1974) 385–388.

[19] O.W. Sørensen, H. Bildsøe, H.J. Jakobsen, Natural-abundance proton-coupled satellite spectra in $^{13}C$ NMR from double selective population transfer. The flip angle effect, J. Magn. Reson. 45 (1981) 325–336.

[20] J. Skibsted, E. Henderson, H.J. Jakobsen, Characterization of calcium aluminate phases in cements by $^{27}Al$ MAS NMR spectroscopy, Inorg. Chem. 32 (1993) 1013–1027.

[21] J. Skibsted, L. Hjorth, H.J. Jakobsen, Quantification of thaumasite in cementitious materials by $^{29}Si\{^{1}H\}$ cross-polarization magic-angle spinning NMR spectroscopy, Adv. Cem. Res. 7 (1995) 69–83.

[22] A.R. Hove, H. Bildsøe, J. Skibsted, M. Brorson, H.J. Jakobsen, Probing crystal structures and transformation reactions of ammonium molybdates by $^{14}N$ MAS NMR spectroscopy, Inorg. Chem. 45 (2006) 10873–10881.

[23] T. Vosegaard, J. Skibsted, H. Bildsøe, H.J. Jakobsen, Combined effect of second-order quadrupole coupling and chemical shielding anisotropy on the central transition in MAS NMR of quadrupolar nuclei. $^{87}Rb$ MAS NMR of $RbClO_4$, J. Phys. Chem. 99 (1995) 10731–10735.

[24] J. Skibsted, S. Rasmussen, D. Herfort, H.J. Jakobsen, $^{29}Si$ cross-polarization magic-angle spinning NMR spectroscopy—an efficient tool for quantification of thaumasite in cement-based materials, Cem. Concr. Comp. 25 (2003) 823–829.

[25] A.E. Moore, H.F.W. Taylor, Crystal structure of ettringite, Acta Crystallogr. B26 (1970) 386–393.

[26] F. Goetz-Neunhoeffer, J. Neubauer, Refined ettringite ($Ca_6Al_2(SO_4)_3(OH)_{12} \cdot 26H_2O$) structure for quantitative X-ray diffraction analysis, Powder Diffrac. 21 (2006) 4–11.

[27] R.A. Edge, H.F.W. Taylor, Crystal structure of thaumasite, $Ca_3Si(OH)_6(SO_4)(CO_3) \cdot 12H_2O$, Acta Crystallogr. B27 (1971) 594–601.

[28] J. Skibsted, N.C. Nielsen, H. Bildsøe, H.J. Jakobsen, $^{51}V$ MAS NMR Spectroscopy: determination of quadrupole and anisotropic shielding tensors, including the relative orientation of their principal-axis systems, Chem. Phys. Lett. 188 (1992) 405–412.